

Comparison of topological classifications of quadratic bosonic excitations with examples

Yan He¹ and Chih-Chun Chien²

¹*College of Physics, Sichuan University, Chengdu, Sichuan 610064, China**

²*Department of physics, University of California, Merced, CA 95343, USA.†*

The topological classifications of quadratic bosonic systems according to the symmetries of the Hamiltonian, the dynamic matrix from the equation of motion, and the effective Hamiltonian from the Lindblad equation are summarized. The Hermitian Hamiltonian leads to a three-fold way table while the non-Hermitian dynamic matrix and effective Hamiltonian lead to a ten-fold way table. The difference comes from the bosonic commutation relation on the particle-hole and chiral symmetries. Moreover, the system-reservoir coupling may cause a system with or without coupling to a reservoir to fall into different classes. We present a 1D bosonic pairing model inspired by the fermionic Kitaev chain to contrast the topological behavior from the Hamiltonian, dynamic matrix, and effective Hamiltonian. In contrast, a 2D Chern insulator is insensitive to the different classifications.

I. INTRODUCTION

Studies of topological insulators and topological superconductors according to the underlying symmetries have led to “periodic tables” that classify various topological systems in different dimensions (see Refs. [1, 2] for a review). For electronic systems, the topological properties are usually analyzed by the band structures because the Fermi-Dirac statistics leads to occupied or unoccupied bands. Since the ground states of bosonic systems correspond to a Bose-Einstein condensate (BEC) of massive bosons or vacuum of massless bosons, topological properties of bosonic systems may be studied in the excited states via the Bogoliubov-de Gennes (BdG) formalism, which has been applied to collective modes of superfluid helium [3] and atomic BEC [4–7], photonics [8], phononics [9], magnons [10–12], magnetoelastic excitations [13], and others [14–17].

While the Hamiltonian of an isolated fermionic or bosonic systems is Hermitian, the transformations of the Hamiltonians with respect to the particle-hole symmetry are different for bosons and fermions in the BdG form [18, 19]. The missing of a minus sign in the bosonic case leads to a smaller number of distinct classes for bosons, reducing the tenfold-way table of fermions to a three-fold way table. Due to the Bose-Einstein statistics, the BdG Hamiltonian and the equation of motion of bosonic excitations may react to a symmetry differently [18–21]. In contrast, the fermion BdG equation does not show such a complication. Explicitly, the time evolution of bosonic excitations follows a non-Hermitian dynamic matrix instead of the Hermitian Hamiltonian due to the underlying commutation relations. Moreover, non-Hermitian properties may be present even when the bosonic Hamiltonian is Hermitian [22]. Under certain conditions, the dynamics of quadratic bosonic sys-

tems may be mapped to more complicated fermionic systems [19, 20].

The second-quantized Hamiltonian of a quadratic fermionic (bosonic) system can be diagonalized by a Bogoliubov transformation with the coefficients forming a unitary (para-unitary) matrix in order to satisfy the anti-commutation (commutation) relations [3]. For bosons, the energy spectrum can be found equivalently from the diagonalization of the dynamic matrix [12, 14]. Importantly, the bosonic dynamic matrix transforms under the particle-hole symmetry in the same way as the fermionic Hamiltonian. Therefore, the tenfold-way classification of fermions applies to bosonic excitations according to their dynamic matrix, despite its non-Hermitian property. Interesting topological properties and invariants of non-Hermitian systems have been reviewed in Refs. [21, 23].

For quantum systems coupled to external reservoirs, the Lindblad equation has been widely used to describe quantum dynamics of open systems [24–26]. There have been many studies of topological properties of open quantum systems [27–32]. By implementing a method known as the “third quantization” for quadratic fermionic systems [33], Ref. [34] provides a classification of the steady states of the Lindblad equation according to the symmetries. Since the third quantization for quadratic bosonic systems has been developed [35] as well, here we analyze the topological classification of open quadratic bosonic systems described by the Lindblad equation. The effective Hamiltonian from the Lindblad equation plays the role of the dynamic matrix in the equation of motion of an isolated system. While non-Hermitian properties will be encountered in the dynamic matrix and effective Hamiltonian of bosons, here we only consider models with real line gaps or models whose complex spectrum can be continuously deformed into some intervals on the real axis. With this constraint, we will not address the full extent of the 38-fold way classification of non-Hermitian models [36]. In our discussion, the symmetry classes of non-Hermitian models will be reminiscent of the ten-fold way classification of Hermitian fermionic models. The classification according to the effective Hamiltonian, inter-

* heyang_ctp@scu.edu.cn

† cchien5@ucmerced.edu

estingly, has the same table as the one according to the dynamic matrix. However, we will show that the system-reservoir coupling of the Lindblad equation can introduce additional subtleties.

By analyzing explicit examples, we will show that bosonic excitations can exhibit topological properties contrasting the different topological classifications according to the Hamiltonian, dynamic matrix, and effective Hamiltonian. For example, the three-fold way classification according to the bosonic Hamiltonian does not have any non-trivial topological class in 1D. In contrast, there are topological classes in 1D according to the ten-fold way classification of the dynamic matrix. Our 1D example is a bosonic pairing model with both s-wave and d-wave pairings. This is in contrast to the fermionic Kitaev chain [37] with p-wave pairing due to the Pauli exclusion principle. For the 1D bosonic pairing model, the classifications of the dynamic matrix and effective Hamiltonian agree if the system-reservoir coupling respects the particle-hole symmetry. In that case, the system shows a quantized Berry phase with periodic boundary condition and localized edge states with open boundary condition. However, if the system-reservoir coupling breaks the particle-hole symmetry, the effective Hamiltonian will lead to a different class from the one of the dynamic matrix. We also present a 2D bosonic Chern insulator that lacks a symmetry, therefore showing similar topological behavior according to the three different classifications.

The rest of the paper is organized as follows. Sec. II summarizes the classifications of quadratic bosonic systems via symmetries and dimensions. The three-fold way table according to the Hamiltonian and the ten-fold way table according to the dynamic matrix from the equation of motion or the effective Hamiltonian from the Lindblad equation are explained. To contrast the difference, Sec. III shows a 1D bosonic pairing model that exhibit different topological behavior according to the different classifications. A 2D bosonic Chern insulator that does not differentiate the various classifications is also discussed. Sec. IV concludes our work. In the Appendix, we summarize some details and subtleties.

II. SYMMETRIES AND CLASSIFICATIONS OF QUADRATIC BOSONIC SYSTEMS

A. Classification according to Hamiltonian

We begin by briefly reviewing the classification of quadratic bosonic systems according to their Hamiltonians. The generic Hermitian Hamiltonian may be written in the BdG form as

$$\mathcal{H} = \sum_{a,b} \psi_a^\dagger H_{ab} \psi_b, \quad H = \begin{pmatrix} A & B \\ B^* & A^* \end{pmatrix}. \quad (1)$$

Here we define $\psi = (a_1, \dots, a_n, a_1^\dagger, \dots, a_n^\dagger)^T$. The matrices A and B satisfy $A^\dagger = A$ and $B^T = B$. The three

| Class | T | C | S | $d=0$ | $d=1$ | $d=2$ | $d=3$ | $d=4$ | $d=5$ | $d=6$ |
|-------|---|---|---|--------------|-------|----------------|----------------|--------------|-------|----------------|
| C | 0 | 0 | 0 | \mathbb{Z} | 0 | \mathbb{Z} | 0 | \mathbb{Z} | 0 | \mathbb{Z} |
| CI | 0 | 0 | 1 | \mathbb{Z} | 0 | \mathbb{Z} | 0 | \mathbb{Z} | 0 | \mathbb{Z} |
| R | + | 0 | 0 | \mathbb{Z} | 0 | 0 | 0 | \mathbb{Z} | 0 | \mathbb{Z}_2 |
| RI | 0 | + | 0 | \mathbb{Z} | 0 | 0 | 0 | \mathbb{Z} | 0 | \mathbb{Z}_2 |
| RII | + | + | 1 | \mathbb{Z} | 0 | 0 | 0 | \mathbb{Z} | 0 | \mathbb{Z}_2 |
| H | - | 0 | 0 | \mathbb{Z} | 0 | \mathbb{Z}_2 | \mathbb{Z}_2 | \mathbb{Z} | 0 | 0 |
| HI | 0 | - | 0 | \mathbb{Z} | 0 | \mathbb{Z}_2 | \mathbb{Z}_2 | \mathbb{Z} | 0 | 0 |
| HII | - | - | 1 | \mathbb{Z} | 0 | \mathbb{Z}_2 | \mathbb{Z}_2 | \mathbb{Z} | 0 | 0 |

Table I. Classification of symmetries and topology of quadratic bosonic systems according to their Hamiltonians. The first column is the labels of the ten classes. The next three columns show the properties of the classes under time-reversal, particle-hole, and chiral symmetries. Here 0 or 1 represents the absence or presence of the symmetry. The + and - signs correspond to $TT^* = \pm 1$ and $CC^* = \pm 1$. The last seven columns show the possible topological phases of the eight classes in different dimensions.

types of symmetry conditions in the first quantized form can be summarized [18] as

$$\text{Time-reversal:} \quad TH^*T^\dagger = H, \quad TT^* = \pm 1, \quad (2)$$

$$\text{Particle-hole:} \quad CH^*C^\dagger = H, \quad CC^* = \pm 1, \quad (3)$$

$$\text{Chiral or sublattice:} \quad SHS^\dagger = H, \quad S^2 = 1. \quad (4)$$

Here T , C and S are three unitary matrices that implement the three aforementioned symmetry conditions. Note that in the first-quantized form, the complex conjugation from time-reversal has already been imposed. The time reversal symmetry has the same effect on both bosonic and fermionic systems. However, there are important differences in the particle-hole symmetry and chiral symmetry between bosonic and fermionic systems. For fermionic systems, we have

$$\text{Particle-hole:} \quad CH^*C^\dagger = -H, \quad CC^* = \pm 1, \quad (5)$$

$$\text{Chiral or sublattice:} \quad SHS^\dagger = -H, \quad S^2 = 1 \quad (6)$$

The minus sign on the right hand side of Eqs. (5) and (6) does not show up in the bosonic cases because of the commutation relations of bosonic operators. The chiral symmetry can be treated as a composition of the time-reversal and particle-hole symmetries. For fermions, it follows that $(CT)H(CT)^\dagger = -H$, where the minus sign comes from the particle-hole symmetry. For bosons, one instead obtains $(CT)H(CT)^\dagger = H$ without the minus sign.

We follow a similar method of Ref. [18] to classify the Hermitian BdG Hamiltonian H . However, our results summarized in Table I are different from those of Ref. [18], and the difference will be explained after we analyze the influence of the symmetries on the topological classification. From Eqs. (2) and (3), the conditions of time-reversal and particle-hole symmetries are of the same form for boson systems. Actually, both of them impose a reality condition on the Hamiltonian. In the

group-theory language, if the reality condition is not satisfied, the Hamiltonian is in a complex representation. If the reality condition is satisfied, the Hamiltonian is in a real or pseudo-real representation, corresponding to $T^*T = \pm 1$. Those three types of representations are equivalent to the class A (no time-reversal symmetry), class AI (time-reversal symmetry with $TT^* = 1$) and class AII (time-reversal symmetry with $TT^* = -1$) in Cartan's category. The three classes of Hamiltonians can also be represented by Hermitian complex, symmetric real, and Hermitian quaternion matrices, respectively. We remark that the classification of the three types of representations are independent of the expansion basis. Therefore, if there are two reality conditions, they must be compatible with each other. When both conditions are present, they determine the same symmetry class as only one reality condition.

Now we turn to the chiral symmetry of bosonic Hamiltonians. The chiral symmetry (4) means that there is a matrix S that commutes with the Hamiltonian. This implies that one can find a non-trivial invariant space in the total Hilbert space, or the Hamiltonian can be put into a block-diagonal form. Therefore, we can focus on only one block, where there is no chiral symmetry any more. In other words, the chiral symmetry of bosonic systems will not change the symmetry class. This is in contrast with the chiral symmetry of fermionic systems, which has an anti-commutation relation with the Hamiltonian.

After clarifying the three types of symmetry conditions, we proceed to analyze the topological classes according to these symmetries. First, if there is no symmetries, the Hamiltonian is a Hermitian complex matrix, which can be labeled as class C. We can impose a chiral symmetry on class C without imposing any reality conditions. This class can be labeled as CI. Both C and CI class have the same classifying space $\mathcal{C}_0 = \mathbb{Z} \times BU$. From this, we obtain the first two rows of Table I. Following class C, we can impose time-reversal symmetry with $T^*T = 1$, particle-hole symmetry with $C^*C = 1$, or both. The three classes are labeled as R, RI, and RII since they all contain real matrices. They also have the same classifying space $\mathcal{R}_0 = \mathbb{Z} \times BO$, from which one can derive the third to fifth rows of Table I. Similarly, one can also impose time-reversal symmetry with $T^*T = -1$, particle-hole symmetry with $C^*C = -1$, or both, which correspond to classes H, HI, and HII containing Hermitian quaternion matrices. The three also have the same classifying space $\mathcal{R}_4 = \mathbb{Z} \times BSp$, giving rise to the last three rows of Table I. The "three-fold way" thus refers to the three distinct classifying spaces. We remark that due to the same reality conditions from time-reversal and particle-hole symmetries on bosonic Hamiltonians, the classification of Table I is different from the results of Ref. [18], which did not fully discern the consequences from the two symmetries.

B. Classification according to dynamic matrix

The dynamic matrix comes from the equation of motion of a quadratic bosonic system with the standard commutation relation: ($\hbar \equiv 1$)

$$i \frac{d\psi_i}{dt} = [\psi_i, H] = \sum_j (\tau_3 H)_{ij} \psi_j. \quad (7)$$

Note that the boson operators satisfy the following canonical commutation relations:

$$[\psi_i, \psi_j^\dagger] = (\tau_3)_{ij}, \quad \psi = (a_1, \dots, a_n, a_1^\dagger, \dots, a_n^\dagger)^T. \quad (8)$$

Here we have introduced $\tau_i = \sigma_i \otimes I$, which applies to the "Nambu space" of bosons [7]. The dynamic matrix is given by

$$H_{\text{dyn}} = \tau_3 H = \begin{pmatrix} A & B \\ -B^* & -A^* \end{pmatrix}. \quad (9)$$

For fermionic systems, the dynamic matrix coincides with the Hamiltonian due to the fermionic anti-commutation relations. In the following, we will show that the dynamic matrix H_{dyn} of bosons may behave differently under symmetry transformations when compared to the Hermitian bosonic Hamiltonian H .

We apply the ideas of Refs. [34, 36] and use the three types of discrete symmetries to classify the dynamic matrix H_{dyn} of a quadratic boson system. We first discuss the time-reversal symmetry, under which the bosonic operators transform as

$$\mathcal{T} a_i \mathcal{T}^\dagger = \sum_j (T)_{ji} a_j, \quad \mathcal{T} a_i^\dagger \mathcal{T}^\dagger = \sum_j (T)_{ji}^* a_j^\dagger. \quad (10)$$

Here \mathcal{T} is the time-reversal operator in the second-quantization form. In the first-quantization form, the time-reversal symmetry of the Hamiltonian gives the condition

$$\begin{pmatrix} T & 0 \\ 0 & T^* \end{pmatrix}^\dagger \begin{pmatrix} A^* & B^* \\ B & A \end{pmatrix} \begin{pmatrix} T & 0 \\ 0 & T^* \end{pmatrix} = \begin{pmatrix} A & B \\ B^* & A^* \end{pmatrix} \quad (11)$$

which in turn determines the transformations of the matrices A and B as

$$T^\dagger A^* T = A, \quad T^\dagger B^* T^* = B. \quad (12)$$

Then, the time-reversal of the dynamic matrix H_{dyn} is

$$\begin{pmatrix} T & 0 \\ 0 & T^* \end{pmatrix}^\dagger \begin{pmatrix} A^* & B^* \\ -B & -A \end{pmatrix} \begin{pmatrix} T & 0 \\ 0 & T^* \end{pmatrix} = \begin{pmatrix} A & B \\ -B^* & -A^* \end{pmatrix}. \quad (13)$$

Although H_{dyn} of a bosonic system may be non-Hermitian, it satisfies the time-reversal symmetry condition $T_1^\dagger H_{\text{dyn}}^* T_1 = H_{\text{dyn}}$ with $T_1 = \text{diag}(T, T^*)$. Therefore, the time-reversal symmetry of the dynamic matrix

| Class | T | C | S | $d=0$ | $d=1$ | $d=2$ | $d=3$ | $d=4$ | $d=5$ | $d=6$ |
|-------|---|---|---|----------------|----------------|----------------|----------------|----------------|----------------|----------------|
| A | 0 | 0 | 0 | \mathbb{Z} | 0 | \mathbb{Z} | 0 | \mathbb{Z} | 0 | \mathbb{Z} |
| AIII | 0 | 0 | 1 | 0 | \mathbb{Z} | 0 | \mathbb{Z} | 0 | \mathbb{Z} | 0 |
| AI | + | 0 | 0 | \mathbb{Z} | 0 | 0 | 0 | \mathbb{Z} | 0 | \mathbb{Z}_2 |
| BDI | + | + | 1 | \mathbb{Z}_2 | \mathbb{Z} | 0 | 0 | 0 | \mathbb{Z} | 0 |
| D | 0 | + | 0 | \mathbb{Z}_2 | \mathbb{Z}_2 | \mathbb{Z} | 0 | 0 | 0 | \mathbb{Z} |
| DIII | - | + | 1 | 0 | \mathbb{Z}_2 | \mathbb{Z}_2 | \mathbb{Z} | 0 | 0 | 0 |
| AII | - | 0 | 0 | \mathbb{Z} | 0 | \mathbb{Z}_2 | \mathbb{Z}_2 | \mathbb{Z} | 0 | 0 |
| CII | - | - | 1 | 0 | \mathbb{Z} | 0 | \mathbb{Z}_2 | \mathbb{Z}_2 | \mathbb{Z} | 0 |
| C | 0 | - | 0 | 0 | 0 | \mathbb{Z} | 0 | \mathbb{Z}_2 | \mathbb{Z}_2 | \mathbb{Z} |
| CI | + | - | 1 | 0 | 0 | 0 | \mathbb{Z} | 0 | \mathbb{Z}_2 | \mathbb{Z}_2 |

Table II. Classification of symmetries and topology of quadratic bosonic systems according to their dynamic matrices. The first column is the Cartan labels of the ten classes. The next three columns show the properties of these classes under time-reversal, particle-hole and chiral symmetries. Here 0 or 1 represents the absence or presence of the symmetry. The + and - signs correspond to $TT^* = \pm 1$ and $CC^* = \pm 1$. The last seven columns show the possible topological phases of the ten classes in various dimensions. The classification according to the effective Hamiltonian produces the same table, but the system-reservoir coupling may change which class a system belongs to.

H_{dyn} of the bosonic system behaves just like a Hermitian fermionic Hamiltonian.

Next, we turn to the particle-hole symmetry of the dynamic matrix. Explicitly, the transformation matrix for the particle-hole symmetry may be taken as $C = \tau_1$, leading to

$$\tau_1 H_{\text{dyn}}^* \tau_1 = -H_{\text{dyn}}. \quad (14)$$

Therefore, we arrived at the same particle-hole symmetry condition as a quadratic fermionic model. The composition of time-reversal and particle-hole symmetries gives rise to chiral symmetry. The condition $(CT)H_{\text{dyn}}(CT)^\dagger = -H_{\text{dyn}}$ behaves in the same way as the fermionic case does. In summary, for the non-Hermitian dynamic matrix H_{dyn} of bosons, the three discrete symmetry conditions are

$$\text{Time-reversal: } TH_{\text{dyn}}^* T^\dagger = H_{\text{dyn}}, \quad TT^* = \pm 1, \quad (15)$$

$$\text{Particle-hole: } CH_{\text{dyn}}^* C^\dagger = -H_{\text{dyn}}, \quad CC^* = \pm 1, \quad (16)$$

$$\text{Chiral or sublattice: } SH_{\text{dyn}} S^\dagger = -H_{\text{dyn}}, \quad S^2 = 1 \quad (17)$$

Since the symmetry conditions are the same as the quadratic fermionic case, the ten-fold way classifications of quadratic fermionic systems [1] can be applied to the dynamic matrix of quadratic boson systems. The classification is summarized in Table II. We remark that the difference between Tables I and II is due to the commutation and anti-commutation relations, causing different particle-hole symmetry conditions for the Hamiltonian. Moreover, particle-hole symmetry is only significant for systems with particle-hole mixing, which arises in systems with pairing effects. Therefore, models without

particle-hole mixing do not discern the difference because particle-hole symmetry has no effect on them.

C. Classification according to effective Hamiltonian

We now turn to open quantum systems of bosons. The Lindblad quantum master equation for the time evolution of the reduced density matrix ρ under the influence of an environment with the Markovian approximation has the expression [24–26] ($\hbar = 1$)

$$i \frac{d\rho}{dt} = \mathcal{L}(\rho) = [\mathcal{H}, \rho] + i \sum_{\mu} \left(2L_{\mu} \rho L_{\mu}^{\dagger} - \{L_{\mu}^{\dagger} L_{\mu}, \rho\} \right) \quad (18)$$

Here L_{μ} are the Lindblad operators modeling the environmental effects on the system. Assuming a quadratic bosonic system with n indices, the generic Hamiltonian is given by

$$\mathcal{H} = \sum_{i,j} \left(a_i^{\dagger} A_{ij} a_j + a_i A_{ij}^* a_j^{\dagger} + a_i B_{ij} a_j + a_i^{\dagger} B_{ij}^* a_j^{\dagger} \right) \quad (19)$$

Here the A and B satisfy $A^{\dagger} = A$ and $B^T = B$. To obtain an exact expression for classifying open bosonic systems, we consider linear Lindblad operators similar to those used in Ref. [35]:

$$L_{\mu} = \sum_j \left(l_{\mu j} a_j + k_{\mu j} a_j^{\dagger} \right). \quad (20)$$

We will focus on open systems that allow a steady-state solution of the Lindblad equation in the long-time limit.

Following Ref. [35] and Appendix A 3, the Liouvillian can be rewritten as

$$\mathcal{L} = \begin{pmatrix} \mathbf{c}' & \mathbf{c} \end{pmatrix} \begin{pmatrix} -X^T & Y \\ 0 & -X \end{pmatrix} \begin{pmatrix} \mathbf{c} \\ \mathbf{c}' \end{pmatrix}. \quad (21)$$

Here $\mathbf{c} = (c_{0,1} \cdots, c_{0,n}, c_{1,1} \cdots, c_{1,n})^T$ and $\mathbf{c}' = (c'_{0,1} \cdots, c'_{0,n}, c'_{1,1} \cdots, c'_{1,n})^T$ are the transformed bosonic operators. We define the following $2n \times 2n$ matrices

$$X = \begin{pmatrix} -A^* & B \\ -B^* & A \end{pmatrix} + \frac{i}{2} \begin{pmatrix} M - N^* & L^T - L \\ L^{\dagger} - L^* & M^* - N \end{pmatrix}, \quad (22)$$

$$Y = \frac{i}{2} \begin{pmatrix} -2iB^* - L^* - L^{\dagger} & 2N \\ 2N^T & 2iB - L - L^T \end{pmatrix}. \quad (23)$$

Here we define three $n \times n$ matrices

$$M_{ij} = \sum_{\mu} l_{\mu i} l_{\mu j}^*, \quad N_{ij} = \sum_{\mu} k_{\mu i} k_{\mu j}^*, \quad L_{ij} = \sum_{\mu} l_{\mu i} k_{\mu j}^*. \quad (24)$$

Ref. [34] proposed that the effective-Hamiltonian X in the open quantum system may play the role of the Hamiltonian in the corresponding isolated system. In general, X is a non-Hermitian matrix. Its $2n$ complex eigenvalues

$\lambda_1, \dots, \lambda_{2n}$ are the counterpart of the eigen-energies of the Hamiltonian of an isolated system.

Following the idea of Ref. [34], we can also use the three types of discrete symmetries to classify the effective Hamiltonian X from the Lindblad equation modeling a bosonic system influenced by the environment. For reasons that will be explained shortly, we decompose the effective Hamiltonian as

$$X = X_0 + X_1 = \begin{pmatrix} -A^* & B \\ -B^* & A \end{pmatrix} + \frac{i}{2} \begin{pmatrix} M - N^* & L^T - L \\ L^\dagger - L^* & M^* - N \end{pmatrix}. \quad (25)$$

The Hamiltonian part gives X_0 and the jump operator part gives X_1 . In what follows, we will first discuss the time-reversal symmetry. The key step is that the linear Lindblad operator satisfies

$$\mathcal{T}_S L_\mu^* \mathcal{T}_S^\dagger = L_\mu. \quad (26)$$

Here \mathcal{T}_S is the time-reversal operator applying to the system only. Recall that the boson operators transform under time reversal as

$$\mathcal{T}_S c_i \mathcal{T}_S^\dagger = \sum_j (T_S)_{ji}^* c_j, \quad \mathcal{T}_S c_i^\dagger \mathcal{T}_S^\dagger = \sum_j (T_S)_{ji} c_j^\dagger. \quad (27)$$

This leads to the following relations

$$\sum_i (T_S)_{ij}^* l_{\mu,j}^* = k_{\mu,i}, \quad \sum_i (T_S)_{ij} k_{\mu,j}^* = l_{\mu,i}, \quad (28)$$

which in turn determine the transformations of the matrices M , N and L as

$$T_S M T_S^\dagger = N^T, \quad T_S^* N T_S^T = M^T, \quad C_S L C_S^T = L^T. \quad (29)$$

Note that both M and N are Hermitian matrices. Then the time-reversal of the jump operator part X_1 is

$$T X_1 T^\dagger = -X_1, \quad (30)$$

$$T = \begin{pmatrix} T_S & 0 \\ 0 & T_S^* \end{pmatrix}, \quad X_1 = \frac{i}{2} \begin{pmatrix} M - N^* & L^T - L \\ L^\dagger - L^* & M^* - N \end{pmatrix} \quad (31)$$

The Hamiltonian part X_0 is similar to the dynamic matrix H_{dyn} , which satisfies the ordinary time-reversal symmetry condition $T X_0^* T^\dagger = X_0$. If we assume the coefficients $l_{\mu,i}$ and $k_{\mu,i}$ in the jump operators are all real numbers, it follows that the jump operator part X_1 also satisfies $T X_1^* T^\dagger = X_1$. Combining these results, we arrived at $T X^* T^\dagger = X$. Therefore, in an open bosonic system described by the Lindblad equation, the time-reversal symmetry condition is applied to the complex conjugate of the effective Hamiltonian X , similar to the case of a fermionic Hamiltonian. However, this is different from the fermionic effective Hamiltonian of the Lindblad equation, where the time-reversal condition is applied to the transpose of the effective Hamiltonian [34].

Now we turn to the particle-hole symmetry. Since X is from the dynamic equation of ρ , we expect its symmetry transformations to be similar to those of H_{dyn} from the

equation of motion rather than the Hermitian bosonic Hamiltonian H . Explicitly, the transformation matrix for the particle-hole symmetry can be taken as $C = \tau_1$, leading to

$$\tau_1 X_0^* \tau_1 = -X_0, \quad \tau_1 X_1^* \tau_1 = -X_1. \quad (32)$$

Therefore, we arrived at the particle-hole symmetry condition $\tau_1 X^* \tau_1 = -X$, which is the same as the quadratic fermionic model. The composition of the time-reversal and particle symmetries gives rise to the chiral symmetry condition $(CT)X(CT)^\dagger = -X$, which is also the same as the fermionic case. In summary, for the non-Hermitian effective Hamiltonian X , the three discrete symmetry conditions are

$$\text{Time-reversal : } T X^* T^\dagger = X, \quad T T^* = \pm 1, \quad (33)$$

$$\text{Particle-hole : } C X^* C^\dagger = -X, \quad C C^* = \pm 1, \quad (34)$$

$$\text{Chiral or sublattice : } S X S^\dagger = -X, \quad S^2 = 1. \quad (35)$$

Since the symmetry conditions are the same as the quadratic fermionic case, the ten-fold way classifications of quadratic fermionic systems [1] can also be applied to the effective Hamiltonian X of quadratic boson systems described by the Lindblad equation with linear Lindblad operators. Therefore, the classification produces the same table as Table II. However, the system-reservoir coupling in the Lindblad equation may lead to an explicit non-Hermitian effective Hamiltonian, causing subtle differences between the same model with and without the coupling to a reservoir.

Before demonstrating the subtle differences in the different classifying schemes by examples, we comment on the physical relevance of the schemes. The classification according to the Hamiltonian (Table I) is suitable for static phenomena of a closed bosonic system. The symmetries and topology properties refer to the system in terms of the original bosonic states. For dynamic processes of a closed bosonic system, the spectrum is determined by the dynamic matrix from the equation of motion, so the classification follows Table II. The quasi-particle states may be used to determine the properties in this case. Unless equilibrium thermodynamics completely determined only by the Hamiltonian (in the micro-canonical ensemble) is considered, the classification according to the dynamic matrix is more common because of its origin in the equation of motion. Finally, if the bosonic system is influenced by an environment and describable by the Lindblad formalism, the classification will follow Table II when one focuses on the effective behavior of the system. The properties may be extracted from the density matrix and its spectrum from the Lindblad equation, which incorporates the effects from the environment.

III. EXAMPLES

A. 1D bosonic pairing model

Our example to contrast the different classifications is a 1D bosonic pairing model inspired by the fermionic Kitaev chain [37]. Since the wavefunction is symmetric for bosons, we can have s-wave and d-wave pairing in the bosonic model rather than the p-wave pairing for spin-polarized fermion superconductors. The Hamiltonian of the 1D bosonic pairing model in real space is given by

$$H = \sum_i \left[iw(a_i^\dagger a_{i+1} + a_{i+1}^\dagger a_i) + \Delta_1 [(a_i^\dagger)^2 + a_i^2] + \Delta_2 (a_i^\dagger a_{i+1}^\dagger + a_{i+1} a_i) \right]. \quad (36)$$

Here a_i and a_i^\dagger are the annihilation and creation operators of bosons on site i . $\Delta_{1,2}$ denote the onsite and nearest-neighbor pairing, respectively. There have been studies on the bosonic analogues of the fermionic Kitaev model [14, 38–40] with pairing between neighbors, and here we study the model with both onsite and nearest-neighbor pairings in closed- and open-system settings. According to Table I, the Hermitian Hamiltonian of the 1D bosonic pairing model does not imply nontrivial topological properties because all classes are trivial in 1D. This is in contrast to the 1D fermionic Kitaev model showing topological properties due to different spin-statistics. We mention there are some subtleties in the classification of the fermion Kitaev chain, leading to different interpretations [1, 34] as summarized in the Appendix. We remark that the 1D bosonic pairing model is different from the bosonic Su-Schrieffer-Heeger (SSH) model [14, 38] because the former has particle-hole symmetry while the latter has chiral symmetry.

In order to find nontrivial topology of the 1D bosonic pairing model according to Table II, we have introduced a purely imaginary hopping coefficient similar to that used in Ref. [40]. Moreover, the bosons do not carry charge. The model may be realized using photonic simulators similar to that discussed in Ref. [40] or cold-atom simulators that can tune the hopping and interactions between bosons [41]. For the 1D bosonic pairing model, the classifications according to the dynamic matrix and the effective Hamiltonian are the same if the Lindblad operators do not break the particle-hole symmetry of the dynamic matrix. For example, we choose the Lindblad operators as

$$L_i = \gamma(a_i + a_{i+1}). \quad (37)$$

In momentum space, we define the "Nambu spinor" for bosons as $\psi = (a_k, a_{-k}^\dagger)^T$. The effective Hamiltonian

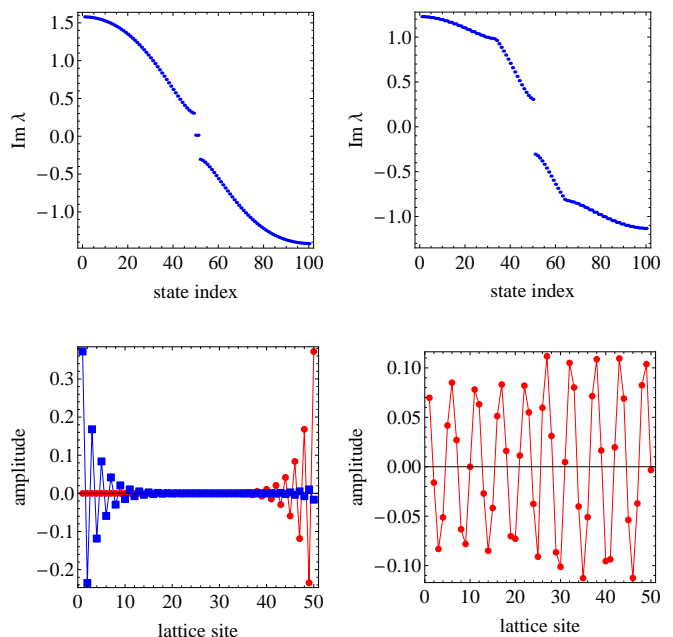


Figure 1. (Top row) Spectrum of the effective Hamiltonian of the 1D bosonic pairing model with open boundary condition for $\Delta_2 = 0.9$ (left) and $\Delta_2 = 0.3$ (right). Here $w = 1$, $\Delta_1 = 0.6$ and $\gamma = 0.2$. (Bottom row) Wave functions of the edge states (left) and a bulk state (right) on a finite lattice of 50 sites.

from the Lindblad equation is given by

$$X = \begin{pmatrix} -iw \sin k & \Delta_1 + \Delta_2 \cos k \\ -(\Delta_1 + \Delta_2 \cos k) & iw \sin k \end{pmatrix} + \frac{i}{2} \begin{pmatrix} 2\gamma^2(1 + \cos k) & 0 \\ 0 & 2\gamma^2(1 + \cos k) \end{pmatrix}. \quad (38)$$

The spectrum of the model is given by

$$\lambda = \pm i\sqrt{w^2 \sin^2 k + (\Delta_1 + \Delta_2 \cos k)^2} + i\gamma^2(1 + \cos k). \quad (39)$$

The topology of this model is characterised by the Berry phase, which is defined for a system with periodic boundary condition as

$$\theta = \int_0^{2\pi} dk \langle u_1 | \frac{\partial}{\partial k} | u_1 \rangle. \quad (40)$$

Here $|u_1\rangle$ is the eigenstate with $\text{Im}\lambda_1 < 0$. For the above model, we find that

$$\theta = \begin{cases} \pi, & \Delta_1 < \Delta_2, \\ 0, & \Delta_1 > \Delta_2. \end{cases} \quad (41)$$

Next, we will study the system with open boundary condition.

For the 1D bosonic pairing model with open boundary condition, we plot the imaginary part of the spectrum of

the effective Hamiltonian in the top row of Figure 1 for $\Delta_2 = 0.9$, $\Delta_2 = 0.3$ and $\gamma = 0.2$, respectively. Both spectra are gapped, but there are two in-gap states connecting the two bands in the upper-left panel. In contrast, there is no in-gap state in the upper-right panel. Those in-gap states are localized edge states, as shown in the lower-left panel of Figure 1. To contrast the wavefunction profiles, we also plot the wavefunction of a typical bulk state showing no localization. The in-gap edge states emerge in the regime where the Berry phase takes the nontrivial value $\theta = \pi$. When $\theta = 0$, the system is topologically trivial and there is no localized edge state.

It can be verified that X respects particle hole symmetry because

$$\tau_1 X^*(-k)\tau_1 = -X(k). \quad (42)$$

Here τ_1 is the first Pauli matrix applying to the Nambu spinor space. Therefore, the effective Hamiltonian of the 1D bosonic pairing model belongs to class D of Table II, which supports a \mathbb{Z}_2 classification in 1D. If some perturbations are applied to the system while the particle-hole symmetry remains intact, we find that a pair of localized states at one end can merge together to acquire some non-zero eigen-energies. Because of this, the number of edge states is not conserved, but the parity of the number of edge states remains the same as long as the particle-hole symmetry is present. Therefore, the topologically nontrivial (trivial) phase corresponds to an odd (even) number of edge states at one end of the chain. We recall that the Berry phase θ is an angle that is defined modulo 2π . This is consistent with the \mathbb{Z}_2 classification according to the Berry phase or the parity of the number of edge states.

In the example, the effective Hamiltonian and the dynamic matrix belong to the same symmetry class. One can change the effective Hamiltonian by using a different set of Lindblad operators. To demonstrate the possibility of having the dynamic matrix and effective Hamiltonian in different classes, we consider the Lindblad operators

$$L_j = \gamma(a_j - ia_{j+1}). \quad (43)$$

Note that for a time-reversal invariant system, we should impose the condition that the coefficients of the Lindblad operators are real numbers. However, the 1D bosonic pairing model does not have time-reversal symmetry. Therefore, we are allowed to use complex numbers in the example. In momentum space, the effective Hamiltonian is given by

$$X = H_{\text{dyn}} + \frac{i}{2} \begin{pmatrix} 2\gamma^2(1 + \sin k) & 0 \\ 0 & 2\gamma^2(1 + \sin k) \end{pmatrix} \quad (44)$$

It can be shown that $\tau_1 X^*(-k)\tau_1 \neq -X(k)$, so the Lindblad operators break the particle-hole symmetry in X even though H_{dyn} respects the symmetry. As a consequence, X belongs to the class A, which is topologically trivial in 1D and different from the classification according to H_{dyn} .

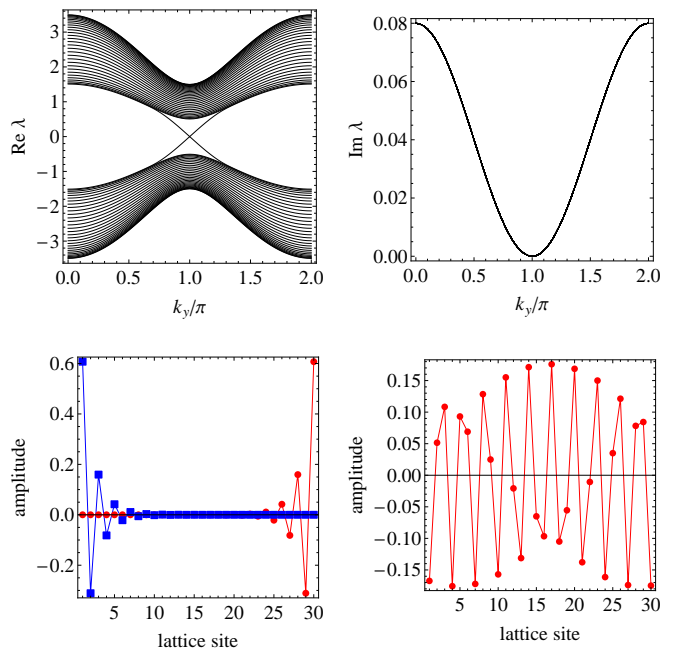


Figure 2. The top row shows the real (left) and imaginary (right) parts of the spectrum of the effective Hamiltonian of the 2D bosonic Chern insulator as a function of k_y for $m = 1.5$ and $\gamma = 0.2$. The bottom row shows the wave functions of the two edge states (left) and a typical bulk state (right) along the direction with open boundary condition.

We would like to mention that effects of spontaneously symmetry breaking on topological systems have been studied in Ref. [42]. Spontaneous symmetry breaking means the ground state of a system does not respect a symmetry of the Hamiltonian. In our classifications of bosonic systems, we analyze the symmetries of the Hamiltonian or its counterpart in open quantum systems. Therefore, the classifications do not take into consideration the broken symmetry in the ground state. Meanwhile, we focus on the excited states rather than the ground state of bosonic systems, so the topological properties and symmetry classes analyzed here may not be affected if spontaneous symmetry breaking is present in the ground state. Nevertheless, adding an explicitly symmetry-breaking term to the Hamiltonian or its counterpart in an open system can change its symmetry classification, and the modified system may have different topological behavior.

B. 2D Chern insulator

Next, we give an example that does not differentiate the three classifications of bosons. The example is a 2D model in class A without any symmetry, which can be thought of as the bosonic counterpart of the fermionic Chern insulator. In real space, the Hamiltonian is given

by

$$\mathcal{H} = \sum_n \left(a_n^\dagger \frac{\sigma_3 - i\sigma_1}{2} a_{n+\hat{x}} + a_n^\dagger \frac{\sigma_3 - i\sigma_2}{2} a_{n+\hat{y}} + h.c. \right) + \sum_n m a_{n,s}^\dagger \sigma_3 a_n. \quad (45)$$

Here $n = (n_x, n_y)$ labels the lattice site on a square lattice. With two orbitals labelled by 1, 2 on each site, the boson operator is defined as $a_n = (a_{n,1}, a_{n,2})^T$. We also define \hat{x} and \hat{y} as the unit vectors along the x and y directions, respectively. There have been studies of the bosonic Chern insulator [8, 10], but here we analyze the model in both closed- and open- system settings. We remark that there is practically no difference between the bosonic and fermionic Chern insulators because the Chern insulator does not have any of the three classifying symmetries. Hence, the complication from the commutation and anticommutation relations does not play a significant role here. As a consequence, there is no difference among the three classifications for the 2D bosonic Chern insulator. Nevertheless, here we present the topological properties of the 2D bosonic Chern insulator described by the Lindblad equation.

The Lindblad operators we considered here have the form

$$L_{n,i} = \gamma(a_{n,i} + a_{n+\hat{y},i}) \quad \text{for } i = 1, 2. \quad (46)$$

Transforming the expression to momentum space, the effective Hamiltonian is given by

$$X = \begin{pmatrix} -H^* + iM/2 & 0 \\ 0 & H + iM^*/2 \end{pmatrix}. \quad (47)$$

The matrices H and M are defined by

$$H = \sum_{j=1}^3 R_j \sigma_j, \quad M = 2\gamma^2(1 + \cos k_y) I_0, \quad (48)$$

$$R_1 = \sin k_x, \quad R_2 = \sin k_y, \quad R_3 = m + \cos k_x + \cos k_y. \quad (49)$$

Here σ_j with $j = 1, 2, 3$ are the Pauli matrices and I_0 is the 2×2 identity matrix. The energy spectrum of the effective Hamiltonian is given by

$$\lambda = \pm \sqrt{R_1^2 + R_2^2 + R_3^2} + i\gamma^2(1 + \cos k_y). \quad (50)$$

The topology of this model may be characterized by the Chern number from the effective Hamiltonian. For the lower band, the Chern number can be related to the 2D winding number as

$$C = -\frac{1}{4\pi} \int d^2k \epsilon_{ijk} \hat{R}_i \cdot (\partial_x \hat{R}_j \times \partial_y \hat{R}_k). \quad (51)$$

For the 2D bosonic model discussed here, the Chern number takes the following values:

$$C = \begin{cases} 1, & 0 < m < 2, \\ -1, & -2 < m < 0, \\ 0, & |m| > 2. \end{cases} \quad (52)$$

For non-Hermitian models, one may introduce more types of topological invariants, such as the vorticity in the energy spectrum [23], defined as

$$v_n = \frac{1}{2\pi} \oint \nabla_{\mathbf{k}} \arg [\lambda_n(\mathbf{k})] \cdot d\mathbf{k}. \quad (53)$$

The vorticity counts the number of exceptional points inside the contour. For the model studied here, however, the contribution from the system-reservoir coupling to the effective Hamiltonian from the Lindblad equation, M , is proportional to the identity matrix due to the choice of the Lindblad operators. Thus, there is no exceptional point, and the vorticity is trivial. For the discussion of Table II, it is more suitable to use the Chern number to characterize the topology. Nevertheless, one can see that this analysis offers another example that different topological classifications can be characterized by different physical quantities.

The Chern number is defined for systems with periodic boundary condition. We further consider the model on a cylinder-shape lattice. Explicitly, we impose open boundary condition along the x axis and periodic boundary condition along the y axis. The resulting Hamiltonian and effective Hamiltonian are still a function of k_y . In Figure 2, we plot the eigenvalue spectrum of the effective Hamiltonian H_{eff} as a function of k_y . We have assumed $m = 1.5$, which corresponds to $C = 1$. In the upper left panel, one can see that there are two chiral edge states connecting the two bands. The edge states are localized at the two open ends of the cylinder. Moreover, there is no non-Hermitian skin effects because the non-Hermitian terms are diagonal. The typical profiles of the edge and bulk states are shown in the bottom of Figure 2. We remark that the system with $C = 0$ in the same cylinder geometry shows no chiral edge state.

IV. CONCLUSION

Depending on the different quantities used in the analyses, quadratic bosonic systems may follow different periodic tables of topological classifications with different interpretations. The difference between the Hermitian Hamiltonian and the non-Hermitian dynamic matrix is from the bosonic commutation relation, particle-hole symmetry, and chiral symmetry, but there is no such difference in fermionic systems with anticommutation relations. Although adding system-reservoir coupling according to the Lindblad formalism does not lead to a different table, the Lindblad operators may change the symmetry properties and cause a model to be assigned to a different class compared to its closed-system counterpart. Our examples have demonstrated the subtle differences in topological properties according to the different classifications and spin statistics. Realizations of the models in physical systems or quantum simulators will illustrate the rich physics of topological bosonic systems.

ACKNOWLEDGMENTS

Y. H. was supported by the Natural Science Foundation of China under Grant No. 11874272 and Science Specialty Program of Sichuan University under Grant No. 2020SCUNL210. C. C. C. was supported by the National Science Foundation under Grant No. PHY-2011360.

Appendix A: Some details

1. Difference between classifications of fermionic and bosonic Hamiltonians

We give a more detailed account for the differences according to the Hamiltonians as follows. The particle-hole symmetry applies to the fermion creation and annihilation operators according to

$$C\psi_a C^{-1} = \sum_b C_{ab}^T \psi_b^\dagger. \quad (\text{A1})$$

Suppose the Hamiltonian in the second quantization form is given by Eq. (1), then the particle-hole symmetry requires that $\mathcal{H} = C\mathcal{H}C^{-1}$. Making use of the transformation of Eq. (A1), we find that

$$\begin{aligned} C\mathcal{H}C^{-1} &= \sum_{a,b,c,d} \psi_a C_{da}^* H_{ab} C_{bc}^T \psi_c^\dagger \\ &= - \sum_{a,b,c,d} \psi_c^\dagger C_{cb} H_{ba}^T C_{ad}^\dagger \psi_d + \text{constant}. \end{aligned} \quad (\text{A2})$$

In the second line, we have used the anti-commutation relations to switch the order of the fermion creation and annihilation operators, causing a minus sign. Comparing the above equation with \mathcal{H} , we arrived at the claimed particle-hole symmetry for the Hamiltonian in the first quantization form as $CH^*C^\dagger = -H$. The same procedure also applies to bosonic Hamiltonians, but the bosonic commutation relations should be used instead of the fermionic anti-commutation relations. Therefore, $CH^*C^\dagger = H$ without a minus sign for bosonic systems.

The absence of the minus sign for the particle-hole and chiral symmetries of bosonic Hamiltonians has important consequences in the topological classification of bosonic systems. We first check the symmetry class A in the fermion ten-fold way classification in zero dimension. The class A has no symmetry, and there is no constraint on the class A Hamiltonian. If we impose chiral symmetry on the class A, we arrived at a new class AIII. The effect of chiral symmetry is to require that the Hamiltonian in class AIII anti-commutes with a certain matrix e_1 . If we treat the matrix e_1 as a basis vector of the Clifford algebra, the process of imposing the chiral symmetry is actually equivalent to the Clifford algebra extension $Cl_0 \rightarrow Cl_1$. Therefore, the classifying space of the class AIII is different from the class A. On the other hand,

there is no minus sign in the relation of chiral symmetry for bosonic Hamiltonians. Imposing chiral symmetry only requires the Hamiltonian to commute with a certain matrix but does not change the classifying space. Therefore, the effects of particle-hole and chiral symmetries according to bosonic Hamiltonians, summarized in Table I, are different from those in fermionic systems following the ten-fold way table. In contrast, the particle-hole and chiral symmetries for the dynamic matrix and effective Hamiltonian of a bosonic system act similarly as their fermionic counterparts, leading to the classifications shown in Table II.

2. Dynamic matrix

If we try to diagonalize the Hermitian BdG Hamiltonian of bosons shown in Eq. (1) as

$$V^\dagger H V = \Lambda \quad (\text{A3})$$

with a diagonal matrix Λ , then the matrix V must satisfy

$$V^\dagger \tau_3 V = \tau_3 \quad (\text{A4})$$

in order to preserve the bosonic canonical commutation relations. The matrix V is actually a para-unitary matrix. We can rewrite Eq. (A3) as

$$V^{-1} (\tau_3 H) V = \tau_3 \Lambda. \quad (\text{A5})$$

The dynamic matrix then has the standard structure of the matrix diagonalization. Here the τ_3 factor compensates for the signature in the definition of the para-unitary matrix.

3. Third quantization of bosons

Following the method of Ref. [35], also known as the ‘‘third quantization’’, one can define a vector space \mathcal{K} that contains the trace class operators and a vector space \mathcal{K}' that contains the unbounded operators, such as physical observables. The elements in \mathcal{K} can be written as a ket $|\rho\rangle$ while the element in \mathcal{K}' can be written as a bra $\langle A|$. The inner product of these spaces is defined as $\langle A|\rho\rangle = \text{tr}(A\rho)$. For a boson operator a , we can define the following left- and right-multiplication maps in \mathcal{K} as follows.

$$a^L |\rho\rangle = |a\rho\rangle, \quad a^R |\rho\rangle = |\rho a\rangle. \quad (\text{A6})$$

According to the cyclic property of trace, these maps apply to \mathcal{K}' as follows.

$$\langle \rho| a^L = \langle \rho a|, \quad \langle \rho| a^R = \langle a\rho|. \quad (\text{A7})$$

In terms the above maps of \mathcal{K} , we can introduce $4n$ maps in the operator space as $c_{\nu,j}$ and $c'_{\nu,j}$ for $\nu = 0, 1$ and $j = 1, \dots, n$ as follows.

$$c_{0,j} = a_j^L, \quad c'_{0,j} = a_j^{\dagger L} - a_j^{\dagger R}, \quad c_{1,j} = a_j^{\dagger R}, \quad c'_{1,j} = a_j^R - a_j^L. \quad (\text{A8})$$

The definition of $c'_{\mu,j}$ is designed to right-annihilate the identity operator, $\langle 1 | c'_{\mu,j} = 0$. One can verify that they satisfy the canonical commutation relations

$$[c_{\mu,i}, c'_{\nu,j}] = \delta_{\mu\nu} \delta_{ij}, [c_{\mu,i}, c_{\nu,j}] = 0, [c'_{\mu,i}, c'_{\nu,j}] = 0. \quad (\text{A9})$$

The super-operator \mathcal{L} in the Lindblad equation (18) may be rewritten as

$$\mathcal{L} = \mathcal{H}^L - \mathcal{H}^R + i \sum_{\mu} \left(2L_{\mu}^L L_{\mu}^{\dagger R} - L_{\mu}^{\dagger L} L_{\mu}^L - L_{\mu}^R L_{\mu}^{\dagger R} \right). \quad (\text{A10})$$

We want to express the above equation in terms of c and c' . To this ends, we reverse the definitions of c and c' and find

$$\begin{aligned} a_j^L &= c_{0,j}, & a_j^{\dagger L} &= c'_{0,j} + c_{1,j}, \\ a_j^R &= c_{0,j} + c'_{1,j}, & a_j^{\dagger R} &= c_{1,j}. \end{aligned} \quad (\text{A11})$$

Together with Eq. (19), it can be shown that

$$\begin{aligned} \mathcal{H}^L &= \sum_{ij} \left[2A_{ij}(c'_{0,i} + c_{1,i})c_{0,j} + B_{ij}c_{0,i}c_{0,j} \right. \\ &\quad \left. + B_{ij}^*(c'_{0,i} + c_{1,i})(c'_{0,j} + c_{1,j}) \right], \end{aligned} \quad (\text{A12})$$

$$\begin{aligned} \mathcal{H}^R &= \sum_{ij} \left[2A_{ij}c_{1,i}(c_{0,j} + c'_{1,j}) + B_{ij}^*c_{1,i}c_{1,j} \right. \\ &\quad \left. + B_{ij}(c_{0,i} + c'_{1,i})(c_{0,j} + c'_{1,j}) \right], \end{aligned} \quad (\text{A13})$$

and

$$L_{\mu}^L = \sum_j \left[l_{\mu j} c_{0,j} + k_{\mu,j} (c'_{0,j} + c_{1,j}) \right], \quad (\text{A14})$$

$$L_{\mu}^{\dagger L} = \sum_j \left[l_{\mu j}^* (c'_{0,j} + c_{1,j}) + k_{\mu,j}^* c_{0,j} \right], \quad (\text{A15})$$

$$L_{\mu}^R = \sum_j \left[l_{\mu j} (c_{0,j} + c'_{1,j}) + k_{\mu,j} c_{1,j} \right], \quad (\text{A16})$$

$$L_{\mu}^{\dagger R} = \sum_j \left[l_{\mu j}^* c_{1,j} + k_{\mu,j}^* (c_{0,j} + c'_{1,j}) \right]. \quad (\text{A17})$$

Applying the results to Eq. (A10), the super-operator \mathcal{L} is now in a quadratic form of c and c' . After some algebra, the final result can be found in Eq. (14) of Ref. [35]. Written in a matrix form, we arrived at Eq. (21).

4. Subtlety of fermionic Kitaev chain

The Hamiltonian of the fermionic Kitaev chain with p-wave pairing is given by

$$H = \sum_i \left[\mu c_i^{\dagger} c_i + w (c_i^{\dagger} c_{i+1} + h.c.) + \Delta (c_i^{\dagger} c_{i+1}^{\dagger} + h.c.) \right]. \quad (\text{A18})$$

Usually, the fermion Kitaev chain is considered to belong to the class D [1]. But if we rewrite the Hamiltonian in terms of Majorana fermions defined as $c_j = a_{2j-1} + ia_{2j}$, then we find

$$\begin{aligned} H &= \frac{i}{2} \sum_j \left(\mu a_{2j-1} a_{2j} + (\Delta - w) a_{2j} a_{2j+1} \right. \\ &\quad \left. + (\Delta + w) a_{2j-1} a_{2j+2} \right). \end{aligned} \quad (\text{A19})$$

If we make transformations $a_{2j-1} \rightarrow a_{2j-1}$ and $a_{2j} \rightarrow -a_{2j}$, then the Hamiltonian gets a minus sign $H \rightarrow -H$. Therefore, in terms of Majorana fermions, this model also satisfies chiral symmetry and belong to the class BDI [34]. In 1D, class BDI has \mathbb{Z} classification. We caution that the difference is at the level of models because the ten-fold classification shown in Table II is based on the symmetries of the system.

-
- [1] C.-K. Chiu, J. C. Y. Teo, A. P. Schnyder, and S. Ryu, *Rev. Mod. Phys.* **88**, 035005 (2016).
[2] T. D. Stanescu, *Introduction to topological quantum matter and quantum computation* (CRC Press, Boca Raton, FL, USA, 2017).
[3] A. L. Fetter and J. D. Walecka, *Quantum Theory of Many-Particle Systems* (Dover Publications, Mineola, NY, 2003).
[4] S. Ronen, D. C. E. Bortolotti, and J. L. Bohn, *Phys. Rev. A* **74**, 013623 (2006).
[5] C. J. Pethick and H. Smith, *Bose-Einstein condensation in dilute gases* (Cambridge University Press, Cambridge, UK, 2008), 2nd ed.
[6] S. Furukawa and M. Ueda, *New J. Phys.* **17**, 115014 (2015).
[7] J. Wang, W. Zheng, and Y. Deng, *Phys. Rev. A* **102**, 043323 (2020).
[8] V. Peano, M. Houde, C. Brendel, F. Marquardt, and A. A. Clerk, *Nat. Comm.* **7**, 10779 (2016).
[9] C. Sanavio, V. Peano, and A. Xuereb, *Phys. Rev. B* **101**, 085108 (2020).
[10] R. Shindou, R. Matsumoto, S. Murakami, and J. I. Ohe, *Phys. Rev. B* **87**, 174427 (2013).
[11] M. Lein and K. Sato, *Phys. Rev. B* **100**, 075414 (2019).
[12] H. Kondo, Y. Akagi, and H. Katsura, *Prog. Theor. Exp. Phys.* **2020**, 12A104 (2020).
[13] S. Park and B. J. Yang, *Phys. Rev. B* **99**, 174435 (2019).

- [14] S. Lieu, Phys. Rev. B **98**, 115135 (2018).
- [15] J. Curtis, G. Refael, and V. Galitski, Ann. Phys. **407**, 148 (2019).
- [16] Y. Akagi, J. Phys. Soc. Jpn. **89**, 123601 (2020).
- [17] H. Y. Ling and B. Kain, *Selection rule for topological amplifiers in bogoliubov de gennes systems* (2021), arXiv: 2011.14935.
- [18] Z. Zhou, L. L. Wan, and Z. F. Xu, J. Phys. A: Math. Theor. **53**, 425203 (2020).
- [19] V. P. Flynn, E. Cobanera, and L. Viola, New J. Phys. **22**, 083004 (2020).
- [20] Q. R. Xu, V. P. Flynn, A. Alase, E. Cobanera, L. Viola, and G. Ortiz, Phys. Rev. B **102**, 125127 (2020).
- [21] Y. Ashida, Z. Gong, and M. Ueda, Adv. Phys. **69**, 249 (2021).
- [22] K. Yokomizo and S. Murakami, *Non-bloch band theory in bosonic bogoliubov-de gennes systems*, arXiv:2012.00439.
- [23] A. Ghatak and T. Das, J. Phys.: Condens. Matter **31**, 263001 (2019).
- [24] S. Haroche and J. M. Raimond, *Exploring the Quantum: Atoms, Cavities, and Photons* (Oxford University Press, Oxford, UK, 2006).
- [25] H. P. Breuer and F. Petruccione, *The theory of open quantum systems* (Oxford University Press, Oxford, UK, 2006).
- [26] U. Weiss, *Quantum Dissipative Systems* (World Scientific Publishing, Singapore, 2012), 4th ed.
- [27] S. Diehl, E. Rico, M. A. Baranov, and P. Zoller, Nat. Phys. **7**, 971 (2011).
- [28] Z. Huang and D. P. Arovas, Phys. Rev. Lett. **113**, 076407 (2014).
- [29] F. Song, S. Yao, and Z. Wang, Phys. Rev. Lett. **123**, 170401 (2019).
- [30] M. Asorey, P. Facchi, and G. Marmo, Open Sys. and Inf. Dyn. **26**, 1950012 (2019).
- [31] S. Bandyopadhyay, S. Bhattacharjee, and D. Sen, *Driven quantum many-body systems and out-of-equilibrium topology* (2021), arXiv: 2103.02279.
- [32] A. McDonald, R. Hanai, and A. A. Clerk, *Non-equilibrium stationary states of quantum non-hermitian lattice models* (2021), arXiv: 2103.01941.
- [33] T. Prosen, New J. Phys. **10**, 043026 (2008).
- [34] S. Lieu, M. McGinley, and N. R. Cooper, Phys. Rev. Lett. **124**, 040401 (2020).
- [35] T. Prosen and T. H. Seligman, J. Phys. A: Math. Theor. **43**, 392004 (2010).
- [36] K. Kawabata, K. Shiozaki, M. Ueda, , and M. Sato, Phys. Rev. X **9**, 041015 (2019).
- [37] A. Kitaev, Annals of Physics **321**, 2 (2006).
- [38] R. Barnett, Phys. Rev. A **88**, 063631 (2013).
- [39] G. Engelhardt, M. Benito, G. Platero, and T. Brandes, Phys. Rev. Lett. **117**, 045302 (2016).
- [40] A. McDonald, T. Pereg-Barnea, and A. A. Clerk, Phys. Rev. X **8**, 041031 (2018).
- [41] S. Vishveshwara and D. M. Weld, *Z2 phases and majorana spectroscopy in paired bose-hubbard chains* (2020), arXiv: 2012.02380.
- [42] A. Raj, N. Banerjee, and T. Das, Phys. Rev. B **103**, 075139 (2021).